Climate Variability in Northwest Greece During the Last Interglacial

M. R. Frogley,[1*†] P. C. Tzedakis,[2†] T. H. E. Heaton[3]

Isotopic and palynological data over the period 115,000 to 135,000 years ago from a lacustrine sequence in northwest Greece show distinct oscillations during the intervals leading into and out of the full interglacial, whereas in between, changes were less pronounced but included a brief fluctuation. After peak interglacial conditions, temperatures decreased and precipitation increased in a series of steps. These data suggest that Eemian climate variability was similar to that of the Holocene both in terms of amplitude and, possibly, of pacing.

The last interglacial (Eemian) provides a measure of natural climate variability during intervals of minimum ice volume that can be compared with Holocene and, potentially, future changes. Results from both marine (*1*, *2*) and terrestrial (*3*–*6*) records have been mixed about the extent of climate instability during this interval, possibly because of differences in their sensitivity and resolution. Here we present a multiproxy climate record spanning the penultimate deglaciation and last interglacial at 90- to 175-year resolution from a lacustrine sequence from Ioannina, northwest Greece. This detailed record enables us to resolve high-frequency events and to address the character of climate change through the last interglacial in this area, as well as the intervals immediately before and after.

The I-284 core (39°45′N, 20°51′E, 472.69 m above sea-level, 319 m overall length) was drilled from the Ioannina basin in 1989. The site is situated on the western flank of the Pindus Mountain Range, ~60 km from the Ionian coast in the region of Epirus. Lake Pamvotis is thought to have occupied the basin since Plio-Pleistocene times, although today it has been substantially reduced in area by artificial drainage. Continual subsidence of the basin floor has resulted in the accumulation of great thicknesses of lacustrine sediments, consisting mostly of calcareous silts and clays.

The age model for the top 200 m of the sequence (*7*) (Fig. 1) was developed by using magnetic susceptibility profiles to link with the pollen record and chronology of an adjacent core (I-249) previously analyzed from the same basin. I-249 spans the last 430,000 years and has been correlated with other long pollen sequences from Europe and from the marine oxygen isotope record (*8*, *9*). Six geomagnetic excursions have been recognized in the top 200 m of I-284, including the globally recognized Blake Event, which has a mean age of 122 ± 10 thousand years (ka) (*10*). The top part of the core was also dated by means of 12 accelerator mass spectrometry (AMS) radiocarbon determinations derived from shells of freshwater molluscs.

The pollen record reflects the immediate response of tree populations to climate changes without migrational lags because of the presence of refugial populations in the vicinity (*8*). The last interglacial in the adjacent I-249 record was characterized by an early peak in *Olea*, a significant expansion of *Carpinus betulus*, and the absence of *Fagus*. This vegetation signature is diagnostic, allowing differentiation from all other forest periods recognized in I-249 (*11*). The new I-284 record (Fig. 2) shows the same palynological features, strengthening correlation of the last interglacial interval in both cores, but at significantly higher resolution (~175 years).

Stable isotopic measurements of fine-grained (<80 μm) calcite were carried out at intervals of approximately every 90 years (Fig. 3). The endogenic nature of the calcite was confirmed by means of detailed scanning electron microscopy analyses (*7*). Ioannina is effectively a hydrologically closed basin, and the factors influencing the $\delta^{18}O$ and $\delta^{13}C$ values of the lake waters are relatively well understood (*12*). In general, we regard higher $\delta^{18}O$ values as indicative of lower precipitation or higher evaporation (that is, lower P/E ratios). Higher $\delta^{13}C$ values are regarded as indicative of lower precipitation, higher organic productivity, or both (*13*).

The combined data (Fig. 3) show that conditions at the end of the penultimate glacial period were characterized by dominance of open vegetation as well as relatively high isotopic values, suggesting a low P/E ratio. A transitional interval of abrupt climate changes occurred between 98.5 and 96.7 m

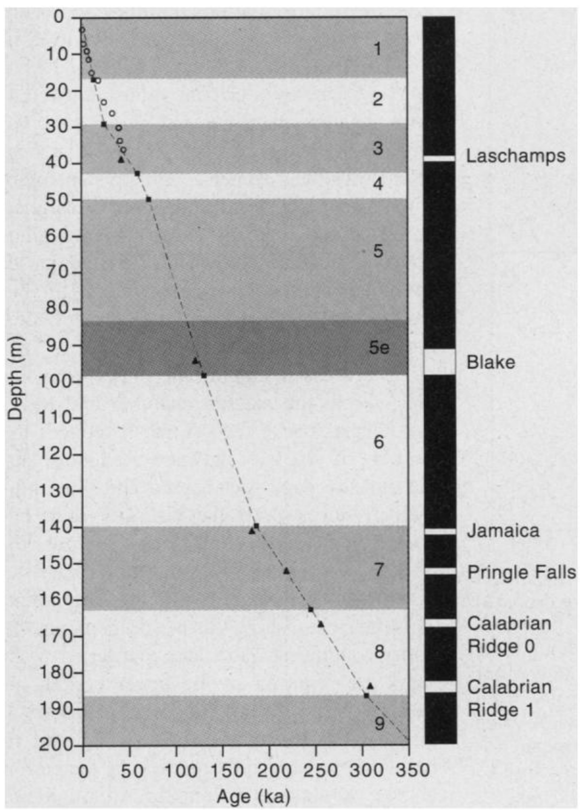

Fig. 1. Chronological framework for the top 200 m of the I-284 sequence. (■) Correlation points with the chronology of I-249 (see text for details). (○) Calibrated AMS radiocarbon determinations. (▲) Mean ages of magnetic polarity events (*10*, *24*). Suggested correlations with marine oxygen isotope stages (*22*) are given.

[1]Godwin Institute for Quaternary Research, Department of Zoology, University of Cambridge, Downing Street, Cambridge CB2 3EJ, UK. [2]Godwin Institute for Quaternary Research, Department of Geography, University of Cambridge, Downing Place, Cambridge CB2 3EN, UK. [3]National Environment Research Council (NERC) Isotope Geosciences Laboratory, Kingsley Dunham Centre, Keyworth, Nottingham NG12 5GG, UK.

*To whom correspondence should be addressed. E-mail: mrf1002@cus.cam.ac.uk

†These authors contributed equally to this work.

(~130 to 127.5 ka), starting with an increase in P/E and an expansion of deciduous *Quercus* populations. This was followed by a shift toward drier environments and more open vegetation. At 96.7 m (127.5 ka) a second, more extensive peak in deciduous *Quercus* values and a change toward more negative $\delta^{18}O$ values signal a reestablishment of wetter conditions and the beginning of the full interglacial.

At 96.2 m (126.8 ka) arboreal pollen (AP) frequencies rise (to 96%), including an increase of Mediterranean elements (*Olea*, *Pistacia*, *Phillyrea*, evergreen *Quercus*), and $\delta^{18}O$ values shift to around −4.8‰. The combination of proxies point to a warmer climate with mild winters and drier (summer drought) conditions. At 95.3 m (~126.1 ka) deciduous *Quercus* frequencies decrease and $\delta^{18}O$ values increase further to −4.3‰, suggesting increased aridity. These values persist to 93.5 m (~124.7 ka), where a stepwise increase in moisture availability is indicated by a decrease in $\delta^{18}O$ values back to about −4.8‰. *Carpinus betulus* frequencies rise significantly and Mediterranean elements decrease (*Olea* virtually disappears), signaling a drop in winter temperatures and an increase in summer precipitation. From around 90.7 m (122.6 ka) moisture availability increased abruptly, as signaled by a drop in $\delta^{18}O$ values (to around −5.2‰) and $\delta^{13}C$ values (to around −1.2‰). Mediterranean elements disappear and deciduous *Quercus* values rise at the expense of *C. betulus*. *Abies* and *Betula* frequencies also increase. The data all point to a decrease in both winter and summer temperatures and an increase in precipitation. Between 88.9 and 88.3 m (~121 to 120.4 ka), an increase in herbaceous frequencies and nonarboreal pollen (NAP) concentrations

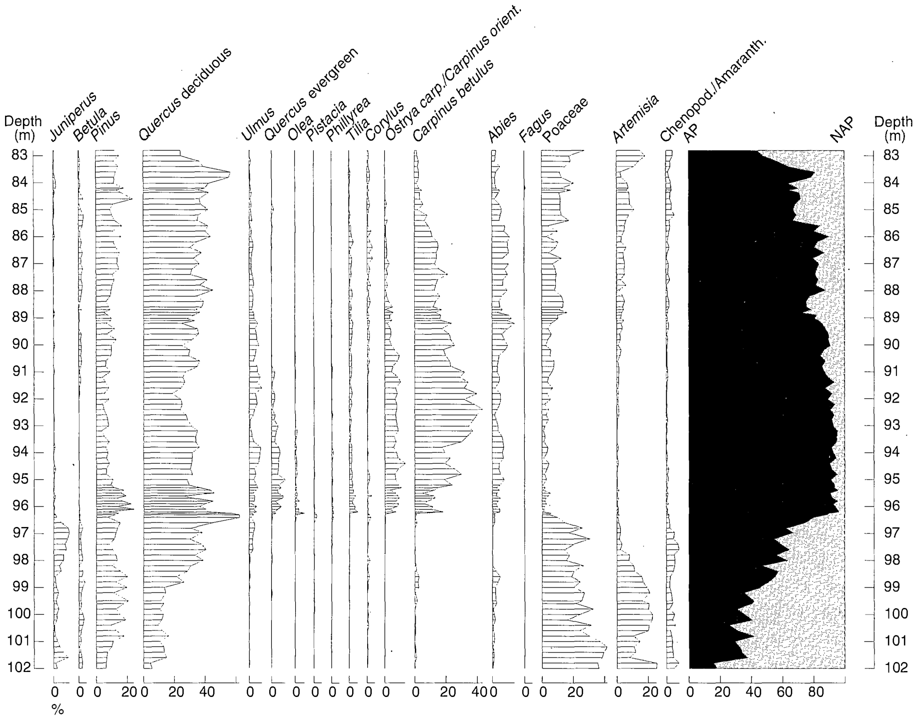

Fig. 2. Pollen diagram showing percentages of selected taxa. The basic calculation sum comprised all pollen of nonaquatic vascular plants with a mean count of 338 ± 34 pollen grains (minimum: 300; maximum: 479). AP: arboreal pollen; NAP: nonarboreal pollen; *Ostrya carp.*: *Ostrya carpinifolia*; *Carpinus orient.*: *Carpinus orientalis*; Chenopod./Amaranth.: Chenopodiaceae/Amaranthaceae. [Analyst: P. C. Tzedakis]

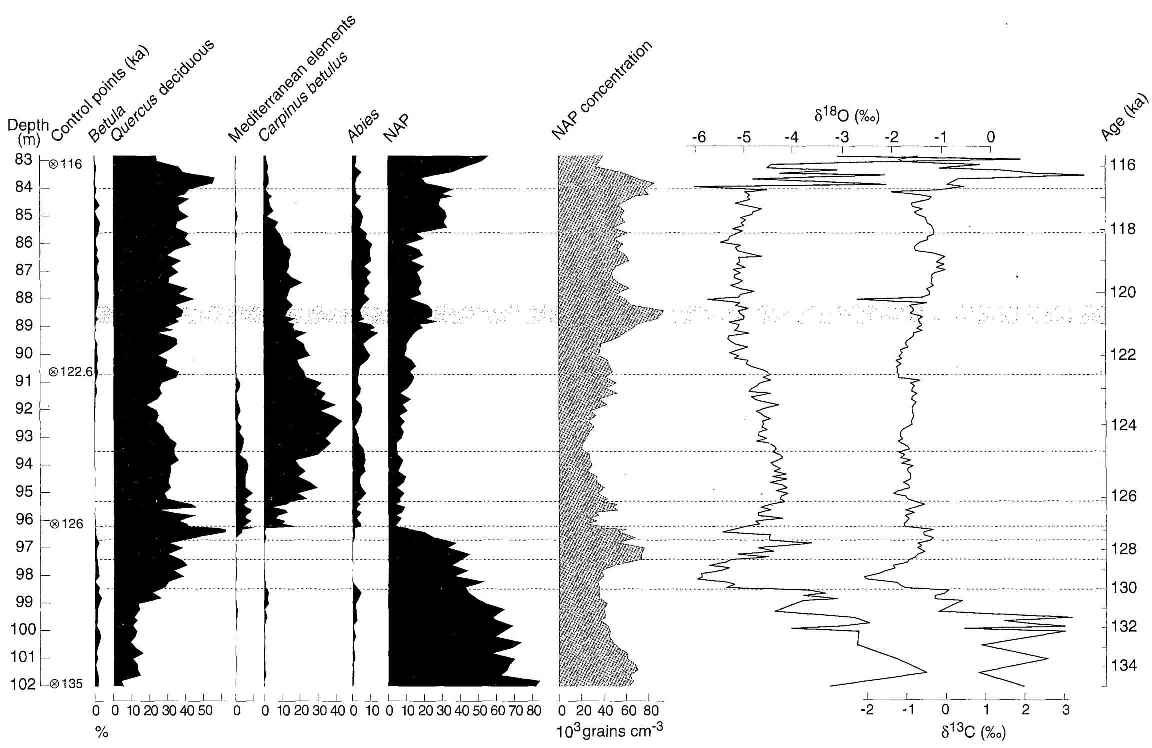

Fig 3. Pollen percentages of selected pollen taxa and groups. Mediterranean elements: evergreen *Quercus*, *Olea*, *Pistacia*, *Phillyrea*. Also shown are NAP concentrations as an indicator of herbaceous biomass; a three-point moving average is used to reduce inherent variability in the data. Stable isotopic results of $\delta^{18}O$ and $\delta^{13}C$ (‰, relative to Vienna Pee Dee belemnite) are also included. All curves are plotted against depth (left-hand axis) and time (right-hand axis) (*25*). Dashed horizontal lines represent the transition between different environmental conditions as determined by the $\delta^{18}O$ record. These transitions correspond to the position of pollen zones produced by numerical zonation techniques (constrained cluster analysis and optimal splitting) run on the entire pollen data set. Shaded band highlights the climatic fluctuation between ~121 and 120.4 ka (see text). Supplemental pollen and isotopic data are available at www.sciencemag.org/feature/data/1042020.shl.

suggests a short expansion of open vegetation. The lack of a marked response in the isotopic record during this event is puzzling, but could be attributed to synchronous drops in temperature and precipitation that produced little change in the P/E ratio. After this, AP frequencies increase again, although not quite reaching pre–88.9 m values. Above ~85.65 m (~118.1 ka), an increase in $\delta^{18}O$ values and NAP frequencies suggests increased aridity. A return to an oscillatory climate is observed after 84 m (~116.7 ka).

The Ioannina data show that the amplitude of changes during the full interglacial was smaller than that of the late-glacial interval and of the transition to the stadial. The late-glacial is a polyphase interval in which temperature and moisture availability oscillated abruptly. It contains an interstadial (~130 to 128.5 ka) followed by a stadial (~128.5 to 127.5 ka) and bears similarities to the two-step deglaciation observed in the marine record (*14*). The transitional period (~116.7 to 116 ka) at the end of the full interglacial also shows significant climate instability, a feature found in other European Eemian isotopic records (*6*).

By comparison, changes within the interglacial proper (127.5 to 116.7 ka) are less pronounced (Fig. 3), but include a brief fluctuation expressed as an increase in open vegetation between ~121 and 120.4 ka. Similar changes have been identified in other records from Greece (*15*) and southern France (*5*, *16*) and all occurred at the same point in the interglacial vegetation succession (that is, after the disappearance of thermophilous elements and the reexpansion of *Betula* and *Pinus*). These changes may also be correlated with an event between 122 and 121 ka in certain North Atlantic marine sequences (*2*), which has been interpreted as evidence for a possible weakening of the thermohaline circulation. However, lack of detailed chronological control for the terrestrial sequences means that synchroneity between the North Atlantic and southern Europe cannot easily be demonstrated.

After peak interglacial conditions at Ioannina, temperatures decreased and precipitation increased. This trend has been discerned across several western and central European Eemian sites (*3*), although changes have generally been considered gradual. However, the Ioannina record suggests that change occurred by a progression of distinct, though subdued, steps at 126.1 (increasingly warmer, drier), 124.7, and 122.6 ka (increasingly cooler, wetter). In the absence of any lithological changes, we do not consider these steps as artifacts of random changes in sedimentation rates. Moreover, transitions in the isotopic curves coincide with changes in the pollen record, thereby suggesting the crossing of important environmental thresholds.

Evidence for extensive Holocene anthropogenic activity at Ioannina complicates attempts to compare directly the climate of the Eemian and the Holocene. Nevertheless, the climate variability during the last interglacial at Ioannina appears to be similar to that seen in Holocene records elsewhere (*17*). Between 130 and 116.7 ka, climate shifts including transitions, steps, and the fluctuation occurred with a mean pacing of 1477 ± 639 years (1542 ± 709 years during the full interglacial). This pattern resembles the 1470 ± 500 year cyclicity in southward advection of ice-bearing waters into the subpolar North Atlantic during the Holocene and Last Glacial (*18*). In view of the uncertainty in our age model, this apparent similarity may have to be viewed with caution, although both data sets suggest that the frequency of change was higher in the earlier part of each interglacial. In addition, the large standard deviation raises doubts over the true periodic nature of these climate shifts. The origin of the Holocene variability has been attributed to a coupled ocean-atmosphere process (*18*) or solar activity (*19*). However, whereas the North Atlantic Holocene records show a series of abrupt oscillations lasting only 100 to 200 years, the Ioannina Eemian record, apart from one fluctuation, indicates a series of shifts leading to the establishment of different climate conditions. It is possible that such shifts may not be a result of quasi-periodic forcing mechanisms, but may arise from a nonlinear response to changes in insolation and represent the crossings between preferred climate states. The transitions between regimes may be characterized by increased instability, expressions of which could be temporary increases in ice rafting in the North Atlantic.

The oscillating phase seen at the end of the Eemian interval at Ioannina does not have any obvious Holocene analog. On the basis of the Eemian age model presented here, the onset of instability appears to have occurred ~10,800 years after the beginning of the full interglacial, which is similar in length to the duration of the Holocene thus far. However, estimates for the duration of the last interglacial on land can vary widely (*20*). Improved chronological control of this interval is necessary if we are to understand the timing and pattern of natural climate variability during the closing stages of an interglacial.

References and Notes

1. J. F. McManus *et al.*, *Nature* **371**, 326 (1994); D. W. Oppo, M. Horowitz, S. J. Lehman, *Paleoceanography* **12**, 51 (1997); J. F. Adkins, E. A. Boyle, L. Keigwin, E. Cortijo, *Nature* **390**, 154 (1997).
2. E. Cortijo *et al.*, *Nature* **372**, 446 (1994); T. Fronval and E. Jansen, *ibid.* **383**, 806 (1996); M. Maslin, M. Sarnthein, J.-J. Knaack, P. Grootes, C. Tzedakis, in *Geological Evolution of Ocean Basins: Results from the Ocean Drilling Program*, A. Cramp, C. J. MacLeod, S. V. Lee, E. J. W. Jones, Eds. (Geological Society, London, 1998), vol. 131, pp. 91–99.
3. W. H. Zagwijn, *Quat. Sci. Rev.* **15**, 451 (1996).
4. M. H. Field, B. Huntley, H. Müller, *Nature* **371**, 779 (1994); R. Cheddadi *et al.*, *Palaeogeogr. Palaeoclimatol. Palaeoecol.* **143**, 73 (1998).
5. N. Thouveny *et al.*, *Nature* **371**, 503 (1994).
6. T. Litt, F. W. Junge, T. Böttger, *Veg. Hist. Archaeobot.* **5**, 247 (1996).
7. M. R. Frogley, thesis, University of Cambridge (1997).
8. P. C. Tzedakis, *Nature* **364**, 437 (1993).
9. ——, *Philos. Trans. R. Soc. London Ser. B* **345**, 403 (1994); P. C. Tzedakis *et al.*, *Earth Planet. Sci. Lett.* **150**, 171 (1997).
10. J. M. Glen and R. S. Coe, *Geol. Soc. Am. Spec. Pap.* **317**, 67 (1997).
11. P. C. Tzedakis and K. D. Bennett, *Quat. Sci. Rev.* **14**, 967 (1995).
12. H.-C. Li and T.-L. Ku, *Palaeogeogr. Palaeoclimatol. Palaeoecol.* **133**, 69 (1997).
13. The lower (>98.5 m) and upper (<84 m) sections of the interval in question (Fig. 3) have carbonate $\delta^{18}O$ and $\delta^{13}C$ values averaging −3.6 and +1.0‰, respectively. The intervening section, however, is characterized by consistently lower values, averaging −5.0‰ ($\delta^{18}O$) and −0.8‰ ($\delta^{13}C$). These are similar in magnitude to those found in the Holocene section of the core (*7*). Because this interval represents the last interglacial, we might anticipate the $\delta^{18}O$ values of meteoric input waters to the lake to be higher than those during the preceding and succeeding glacial periods (*21*). The fact that the change in $\delta^{18}O$ of the Ioannina lake water, as recorded by the endogenic carbonate, occurs in the opposite direction (a glacial to interglacial decrease of ~1.4‰) suggests that average interglacial conditions in the catchment were characterized by significantly higher P/E ratios. This interpretation is also supported by the mollusc and ostracod faunal records, which indicate a progressive increase in lake depth over the interglacial interval (*7*). In addition, increased inflow could lead to the higher carbonate content and decreased $\delta^{13}C$ values observed during the interglacial (*12*).
14. M. Sarnthein and R. Tiedemann, *Paleoceanography* **5**, 1041 (1990).
15. P. C. Tzedakis, *J. Geol. Soc.* **156**, 425 (1998).
16. J. -L. de Beaulieu and M. Reille, *Veg. Hist. Archaeobot.* **1**, 233 (1992).
17. R. B. Alley *et al.*, *Geology* **25**, 483 (1997); J. C. Stager and P. A. Mayewski, *Science* **276**, 1834 (1997); U. von Grafenstein, H. Erlenkeuser, J. Müller, J. Jouzel, S. Johnsen, *Climate Dyn.* **14**, 73 (1998); R. Cheddadi, H. F. Lamb, J. Guiot, S. van der Kaars, *ibid.*, p. 883; U. von Grafenstein, H. Erlenkeuser, A. Brauer, J. Jouzel, S. Johnsen, *Science* **284**, 1654 (1999).
18. G. Bond *et al.*, *Science* **278**, 1257 (1997).
19. B. van Geel *et al.*, *Quat. Sci. Rev.* **18**, 331 (1999).
20. H. Müller, *Geol. Jahrb.* **A21**, 149 (1974); G. Kukla, J. F. McManus, D.-D. Rousseau, I. Chuine, *Quat. Sci. Rev.* **16**, 605 (1997).
21. K. Rozanski, *Chem. Geol. Isotope Geosci. Sect.* **52**, 349 (1985); W. Dansgaard *et al.*, *Nature* **364**, 218 (1993).
22. D. G. Martinson *et al.*, *Quat. Res.* **27**, 1 (1987).
23. R. Cheddadi and M. Rossignol-Strick, *Paleoceanography* **10**, 291 (1995).
24. C. G. Langereis, M. J. Dekkers, G. J. de Lange, M. Paterne, P. J. M. van Santvoort, *Geophys. J. Int.* **129**, 75 (1997).
25. The age model for this interval is based on linear interpolation between four control points. The lower (102 m) point, representing the maximum expansion of open vegetation after which NAP percentages begin to decrease, is assigned an age from the SPECMAP marine chronology (*22*) for the penultimate glacial maximum (event 6.2: 135 ka). The next point (96.2 m) refers to the rise of *Olea*, *Pistacia*, and *Phillyrea*, representing a phase of expansion of Mediterranean vegetation elements that characterizes the early part of the Eemian across southern Europe (*9*). Palynological investigations from marine cores in the eastern Mediterranean Sea also record this event as occurring contemporaneously with the deposition of sapropel S5 (*23*). The initiation of deposition of S5 is astronomically dated to about 126.8 ka (1 ka after

the maximum insolation anomaly), and this age is used here. The third point (90.7 m) refers to the decline of Mediterranean elements and is assigned an age of 122.6 ka (event 5.51 of the SPECMAP time scale) on the basis of joint pollen and isotopic data from marine cores (*23*). Finally, the uppermost point (83.2 m), after which NAP percentages begin to exceed 50%, represents the transition from the last interglacial to the ensuing stadial and is assigned an age for the MIS 5e/5d boundary of ~116 ka (*22*).

26. We thank R. C. Preece, T. C. Atkinson, and M. R. Chapman for comments and S. Boreham and H. Sloane for technical advice and assistance. We are grateful to the director-general and the staff at the Department of Energy Resources of the Institute of Geology and Mineral Exploration in Athens (particularly Y. Broussoulis) for their cooperation and for making the core available. M.R.F. acknowledges a NERC Studentship and a Fellowship from St. John's College, Cambridge; P.C.T. acknowledges a NERC Advanced Fellowship and a Fellowship from Robinson College, Cambridge.

24 May 1999; accepted 28 July 1999

Iron Isotope Biosignatures

Brian L. Beard,[1]* Clark M. Johnson,[1] Lea Cox,[2] Henry Sun,[2] Kenneth H. Nealson,[2] Carmen Aguilar[3]

The $^{56}Fe/^{54}Fe$ of Fe-bearing phases precipitated in sedimentary environments varies by 2.5 per mil ($\delta^{56}Fe$ values of +0.9 to −1.6 per mil). In contrast, the $^{56}Fe/^{54}Fe$ of Fe-bearing phases in igneous rocks from Earth and the moon does not vary measurably ($\delta^{56}Fe = 0.0 \pm 0.3$ per mil). Experiments with dissimilatory Fe-reducing bacteria of the genus *Shewanella algae* grown on a ferrihydrite substrate indicate that the $\delta^{56}Fe$ of ferrous Fe in solution is isotopically lighter than the ferrihydrite substrate by 1.3 per mil. Therefore, the range in $\delta^{56}Fe$ values of sedimentary rocks may reflect biogenic fractionation, and the isotopic composition of Fe may be used to trace the distribution of microorganisms in modern and ancient Earth.

Fractionation of light stable isotopes such as C, O, N, and S is controlled by inorganic processes related to temperature changes and phase transitions, and by biological processes (*1*). This dual control can make it difficult to interpret the origin of isotopic differences in rocks. For example, excursions in $\delta^{13}C$ values in deep-sea sediments can be interpreted as a function of changes in the productivity of the oceans or the partial pressure of CO_2 of the atmosphere (*2*). In contrast, intermediate-mass elements such as Fe may not be fractionated substantially by inorganic processes because the relative mass difference between Fe isotopes is less than that of C, O, N, or S isotopes. However, biological processes may produce measurable Fe-isotopic fractionation because the metabolic processing of Fe involves a number of steps, such as transport across membranes and uptake by enzymes (*3*), that may fractionate isotopes.

Few studies have documented biological fractionation of transition metal elements (*4*) because of the difficulty of measuring precisely the isotopic ratios of transition metals (*5*). Thermal ionization mass spectrometry (TIMS) can produce high-precision isotope ratio measurements of these metals and, in the case of Fe, is not subject to large interferences by Ar-containing species (for example, $^{40}Ar^{16}O$ and $^{40}Ar^{14}N$), as is inductively coupled plasma mass spectrometry. However, TIMS produces large mass-dependent isotope fractionations during the course of a measurement, which must be corrected before the natural isotopic composition of a sample can be determined. Previous attempts to correct instrumental, mass-dependent isotopic fractionation of Fe used an empirical approach that produced data with a 1σ precision of only 2 to 3 per mil for $^{56}Fe/^{54}Fe$ (*6*), an uncertainty that exceeds the range in nature. Here we used a mixed double spike to correct for instrumental mass bias (*7–9*). With the use of this technique, it is possible to make Fe isotope ratio measurements that are precise to ±0.2 to 0.3 per mil (1σ) for $^{56}Fe/^{54}Fe$. We report Fe-isotopic ratios in conventional per mil notation:

$$\delta^{56}Fe = [(^{56}Fe/^{54}Fe)_{measured}/(^{56}Fe/^{54}Fe)_{E\text{-}M} - 1] \times 1000$$

where $(^{56}Fe/^{54}Fe)_{E\text{-}M}$ is the average $^{56}Fe/^{54}Fe$ measured for 15 terrestrial igneous rocks, ranging in composition from peridotite to rhyolite, and five high-Ti lunar basalts. The average $^{56}Fe/^{54}Fe$ measured for the Earth-moon system is 15.7028 (*7*). Terrestrial and lunar rocks comprise an isotopically homogenous igneous iron reservoir that is thought to represent the bulk isotopic composition of Earth and the moon.

Two sets of experiments were performed to determine the magnitude of Fe-isotopic fractionation that might be produced by microorganisms. Experiment 1, run in duplicate at the University of Wisconsin–Milwaukee (U.W.-Milwaukee), used *S. algae* (strains BCM 8 and BrY) grown on a ferrihydrite substrate in an LM growth medium (*10*). After inoculation of the ferrihydrite + growth medium solution with the cells, the bacteria were allowed to reduce Fe for 8 hours. One run was contained in a 10,000 molecular weight dialysis bag (ferrihydrite + cells + growth medium) suspended in a 100-ml flask of LM growth medium, which allowed the ferrihydrite and cells to be removed from the growth medium. The other run was done in a 100-ml flask, followed by separation of the ferrihydrite and cells from the growth medium + hydrolyzed Fe(II), by filtration. Ferrous iron in the growth medium solution was precipitated by adding ultrapure ammonia, to increase the pH to 9 to 10 immediately after the solution was exposed to the atmosphere, and then allowed to sit for 3 to 5 days. Abiological control experiments were run in parallel; addition of ammonia did not precipitate any iron, confirming that no substantial amount of ferrous Fe was generated. The ammonia precipitation procedure effectively removes the Fe(II) from the growth medium as a ferric oxyhydroxide, which was centrifuged and washed three times in doubly distilled H_2O. The precipitate was dissolved in 6 M HCl, after which followed chemical processing and isotopic analysis with the methods of (*7, 8*).

Experiment 2, performed at the Jet Propulsion Laboratory (JPL), used *S. algae* BrY grown on ferrihydrite in an LB growth medium (*11*). Three runs were made, harvesting Fe 13, 15, and 23 days after inoculation, which produced Fe(II) contents of 5.5, 11.1, and 35.6 parts per million (ppm) Fe, respectively (*12*). Each solution was sterilized with a 0.2-μm filter. Reacted ferrihydrite from runs 2 and 3 was saved for Fe isotope analysis. Splits (50 ml) of the Fe(II) solutions were evaporated to dryness and the organic material combusted in quartz crucibles in a muffle furnace at 700°C for 8 hours. The remaining solids were dissolved in 6 M HCl and processed for Fe isotope analysis as in (*7, 8*). A parallel set of 50-ml aliquots from each run was processed, for comparison with the samples that were combusted, where Fe was harvested as an oxyhydroxide using 10 ml of 30% H_2O_2 in ammonia to bring the pH to 9 to 10. The precipitated Fe oxyhydroxide was treated in the same manner as in the U.W.-Milwaukee experiments. The JPL experiments also included an abiological control, which was harvested by the H_2O_2 + ammonia precipitation technique, as well as by the evaporation and combustion technique.

The high levels of Fe(II) that are produced

[1]Department of Geology and Geophysics, University of Wisconsin-Madison, 1215 West Dayton Street, Madison, WI 53706, USA. [2]Jet Propulsion Laboratory, MS 183-301, 4800 Oak Grove Road, Pasadena, CA 91109–8009, USA. [3]Institute for Great Lakes Study, University of Wisconsin-Milwaukee, 600 East Greenfield Avenue, Milwaukee, WI 53204, USA.

*To whom correspondence should be addressed. E-mail: beardb@geology.wisc.edu